Published as: Lanckriet, S., Schwenninger, J. L., Frankl, A., Nyssen, J., 2015. The Late-Holocene geomorphic history of the Ethiopian Highlands: Supportive evidence from May Tsimble. Catena 135, 290–303.

ABSTRACT

Alluvial sedimentary archives contain important geochronological and paleo-environmental information on past geomorphic processes in semi-arid regions. For North Ethiopia in particular, flashflood sediments transported by ephemeral streams can provide interesting chronological information on Late-Holocene land degradation, whether or not impacted by climate or land cover changes upstream. Here we compare geomorphic records with independent regional records of rainfall regime changes, land use/cover changes and macrohistory, supported by optically stimulated luminescence (OSL) dates for fluvial activity at a sediment sequence in the May Tsimble catchment, in the Northeastern Highlands. We identified two degradation periods over the past 4000 years, one broadly from 1500-500 BCE and one from 500 CE onwards. At least one prior incision phase is responsible for the stabilized gullies that can be seen on photographs around 1900 and another incision phase is dated to the late 20th century. Based on all datasets, we (re-)interpret the geomorphic history of the Highlands. Land degradation is dominantly determined by a human impact, although the impact of this human influence does get amplified during dry spells.

Keywords: alluvial sediments – hydrogeomorphology – land degradation – political ecology

1. INTRODUCTION

In drylands worldwide, land degradation and desertification put severe pressure on food production and food security (Goudie, 2013). Deciphering the Late-Holocene history of land degradation forms an important aspect of a full understanding of the relative impacts of its (long-term) driving factors, including climate, land cover changes and sociopolitical impacts. River sediment yield and cycles of stream incision and deposition can provide suitable proxies for the intensity of land degradation (Avni, 2006; Lanckriet et al., 2014a; Vanmaercke et al., 2011, 2014), since erosion by ephemeral streams in drylands constitutes between 50 to 80% of all sediment production (Poesen et al., 2002). These sediments get accumulated or aggraded in alluvial floodplains, stored as valuable archives on Late-Holocene land degradation (Broothaerts et al., 2013).

We turn to the North Ethiopian Highlands, where severe gullying is indeed a major cause of land degradation (Frankl et al., 2013; Nyssen et al., 2004). Here, dense gully networks are present in the landscape (Frankl et al., 2011). However, few datasets exist on the Late-Holocene evolution of degradation processes in this region. Nyssen et al. (2009) showed that intense degradation occurred at least since the late 19th century, inferring a rather gradual environmental change. The oldest gully activity phase identifiable using repeat photography was a phase of relatively stable gullies that was evidenced on historical photographs of 1868-1936, lasting until the 1960s (Frankl et al., 2011, 2013). Hence, at a regional scale, Frankl et al. (2011) have identified one cut-and-fill cycle since the second half of the 19th century, and identified an earlier one based on the interpretation of historical photographs. Although at least one cycle had existed before 1868, the status of the gully networks that developed (and stabilized) before 1868 is unclear, since other hydrogeomorphic information on gullies before this period is lacking and no reliable direct sediment dating is available yet. A thorough chronological study on older cycles was never performed. It is hitherto not known if there is a

continuous acceleration of geomorphic processes at longer time scales in the North Ethiopian Highlands. However, it is likely that the current cycle is the last of a series of cut-and-fill cycles, since driving factors were equally active during the previous centuries (Lanckriet et al., 2014a).

The sediments deposited by flashfloods in aggraded paleo-channels or preserved in terraces can also provide information on the driving factors of ephemeral stream systems. A literature review (Lanckriet et al., 2014a) shows that vegetation cover and climate changes are the two dominant driving factors of gullying named in most of the studies worldwide. Indeed, in the Ethiopian Highlands a decreasing vegetation cover upstream leads to intensified stream erosion and increased sediment supply downstream (aggradation) (Frankl et al., 2011). Simultaneously, Carnicelli et al. (2009) discuss the possibility that in the Ethiopian Highlands increased runoff under a wetter climate leads to overall gully incision; while decreased runoff and sediment transport capacity under a dryer climate would increase the sediment supply downstream (aggradation). This is in line with the findings by Pelletier et al. (2011), who indicate that because of decreased runoff volumes, a drier climate is less capable of facilitating stream incision.

Obtaining reliable chronologies of stream activity is a key element for the acquisition of accurate environmental information on early land degradation intensities. This can be a particularly difficult task in drylands such as North Ethiopia, partly because ephemeral stream sediments are often not containing convenient organic matter to use for radiocarbon dating. Exceptionally, Machado et al. (1998) obtained an alluvial chronology for three sites in North Ethiopia using radiocarbon dating on buried paleosols. Optically stimulated luminescence (OSL) dating of flash flood sediments can be a valuable alternative, although it can suffer

from insufficient or heterogeneous bleaching (Bourke et al., 2003; Arnold et al., 2007). OSL dating of relatively young sediments is also difficult given a low signal-to-noise ratio and processes such as thermic transfer (Costas et al., 2012; Eipert, 2004). A literature review regarding luminescence dating of ephemeral stream deposits all over the world (Table 1) shows that it is often possible to extract OSL ages from these flashflood sediments, although bleaching properties can strongly impact the level of accuracy. The review shows that most studies focusing on ephemeral stream sediments are dealing with heterogeneous bleaching properties (13 out of 20 studies). Solutions to this problem are given by residual age calculation, analysis of single grains or small aliquots and/or by applying the Minimum Age Model (MAM) of Galbraith et al. (1999) (7 out of the 13 studies). In this model, the (log) equivalent doses D_e form a random sample from a mixed truncated normal distribution. For (young) fluvial sediment samples, (un)logged MAM-3 or MAM-4 models are often preferred over other equivalent dose decision models, such as the Central Age Model, the L-5% model or the Finite Mixture Model (Bailey and Arnold, 2006). Some studies report bleaching properties dependent on grain size, with the coarsest quartz grains (e.g. 212-250 µm) yielding the lowest values of D_e (Wallinga, 2002; Alexanderson, 2007). Others employ a residual age calculation from a modern sample to empirically determine the age-overestimation due to poor bleaching (Table 1), as it is a very simple and straightforward method.

TABLE 1

The aim of this study is to (re-)assess the Late-Holocene environmental evolution of the North Ethiopian Highlands using alluvial sedimentary archives. This can be done (i) by comparing geomorphic chronologies with other paleo environmental records from the region; and (ii) by bringing supportive evidence from dating of aggradation in a suitable catchment.

98 ## 2. METHODS

99 ### 2.1 Geology of the study area and reconnaissance survey

100 The North Ethiopian Highlands drain towards the African Rift and the Tekeze-Nile rivers.
101 The region is composed of Precambrian metavolcanics and Mesozoic sedimentary rocks,
102 which include (from lower to upper) Adigrat sandstone, Antalo limestone, Agula shales, and
103 Amba Aradam sandstone. These sedimentary rocks were intruded by younger (Cenozoic)
104 dolerite dykes and sills and on top Tertiary basalts are found (Merla et al., 1979). Except for
105 Enticho sandstone and the Adaga Arbi tillites, Paleozoic rocks are rare (Bussert and Schrank,
106 2007).

107 As it is wise to start with a mineralogical reconnaissance survey before turning to the
108 luminescence procedures (Duller, 2008), several sites where observations had been done on
109 the presence of old debris cones or (filled) paleo channels (Frankl et al., 2013) were visited
110 during December 2012. Samples were taken at approximately 0.5 m depth in profile pits at
111 interesting sediment accumulations in the main gullies, identified during walks around their
112 catchments. Mineralogy of the sandy fraction (250-106 μm) was studied by microscope
113 (Table 2). In the catchments of Nebelet and May Tsimble, in the uplands of the Rift Valley
114 escarpment, sufficient quartz was present in the sediment samples (Table 2). As the stream
115 system of May Tsimble is much more extensive compared to that of Nebelet, another
116 fieldwork focused on the May Tsimble catchment. Downstream of the large upper stream
117 network in May Tsimble (Figure 1), an interesting sequence of terraces was identified in
118 September 2013.

119 TABLE 2

120 FIGURE 1

2.2 Review of paleo-environmental datasets

Available alluvial records were compared with independent paleo-environmental datasets from the region.

2.2.1 Hydroclimatic records

Two high-quality records of rainfall regime changes have been derived from sediment cores from Lake Ashenge (focus on BCE) (Marshall et al., 2009) and from Lake Hayk (focus on CE) (Lamb et al., 2007). At Lake Ashenge, the hydroclimatic record was derived from (i) diatom species analysis, (ii) diatom-inferred estimation of conductivity and (iii) stable oxygen and carbon isotope analysis of carbonates. At Lake Hayk, a similar methodology was used.

2.2.2 Land cover records

High-quality information of land cover changes was derived from pollen analysis of cores from Lake Hayk (Darbyshire et al., 2003) and pollen identification from Lake Ashenge (Marshall et al., 2009). At Lake Hayk, land cover was reconstructed from a combination of (i) pollen counting, (ii) pollen-assemblage zoning and (iii) the analysis of microscopic and macroscopic charcoal fragments.

2.2.3 Macrohistory

Macrohistory – the long-term patterns of political, economic and social change (Collins, 1999) – was derived from groundwork studies on the pre-Axumite period (Phillipson, 2009), on the Axumite period (Phillipson, 2012) and on the post-Axumite dynasties (Pankhurst, 1990). All reported dates are expressed in (B)CE ((Before) Common Era), including the calibrated radiocarbon dates derived from literature.

2.3 Supportive OSL evidence complemented with semi-structured interviews

2.3.1 Fieldwork, interviews and sampling

The May Tsimble catchment comprises a large ephemeral stream system about 20 km to the southeast of Mekelle, the capital city of the Tigray region in northern Ethiopia. Rainfall in the catchment likely ranges between 400-800 mm because of regional rainfall gradients and high relief. The sampling site (at around 2000 m a.s.l.) is located 6-8 km from the source of the stream, which is located in mountains rising to 2550 m a.s.l. Very recent flood deposits were observed at a height of 1.70 m above the channel floor, indicating the occurrence of individual flashflood events. The main stream is confined to a single ~3-m deep channel, with pool-riffle sequences cut into the alluvium until it reaches the underlying Antalo limestone bedrock. The channel width is about 9 m near the village of Lahama. The identified sequence of terraces is located at the left bank of the May Tsimble stream, along an abandoned palaeochannel next to the active channel (Figure 2). Topographic heights and positions of all terraces were recorded (Figure 2). In line with the method developed by Nyssen et al. (2006), we performed semi-structured interviews with 6 farmers, focusing on the stream evolution and the timing and processes of the changes in morphology. Samples for OSL dating were extracted from the terrace walls and in two profile pits (Figure 2), in line with the recommendations of Duller (2008). For instance, we sampled at sandy lenses, used opaque tubes and wrapped them in thick black plastic. The sampled alluvial terraces are, similar to the contemporary bedload, mainly consisting of large sandy lenses with pebbles of dolerite, sandstone and limestone in-between. The sampling locations were chosen to include all alluvial terraces, in order to investigate the possibility of a complex terrace genesis instead of floodplain aggradation.

166 In order to estimate residual ages, one subrecent sample was collected from a sandy alluvium
167 recently deposited just upstream of a new check dam built in 2010, 0.5 km upstream of the
168 studied cross-section (Figure 3).

169 FIGURE 2

170 FIGURE 3

171

172 *2.3.2 Luminescence procedures*

173 Measurements were performed at the Oxford University Luminescence Dating Laboratory on
174 sand-sized quartz (180-255µm) extracted from the seven samples (X6431-X6437) using
175 standard preparation techniques including wet sieving, HCl (10%) treatment to remove
176 carbonates, HF treatment (48%) to dissolve feldspathic minerals and heavy mineral separation
177 with sodium polytungstate. All samples were measured in automated Risø luminescence
178 readers (Bøtter-Jensen, 1988, 1997, 2000) using a SAR post-IR blue OSL measurement
179 protocol (Murray and Wintle, 2000; Banerjee et al., 2001; Wintle and Murray, 2006). Dose
180 rate calculations are based on the concentration of radioactive elements (potassium, thorium
181 and uranium) within the samples and were derived from elemental analysis by Induced
182 Coupled Plasma Mass Spectroscopy / Atomic Emission Spectroscopy using a fusion sample
183 preparation technique. The final OSL age estimates include an additional 2% systematic error
184 to account for uncertainties in source calibration. Dose rate calculations are based on Aitken
185 (1985). These incorporated beta attenuation factors (Mejdahl, 1979), dose rate conversion
186 factors (Adamiec and Aitken, 1998) and an absorption coefficient for the water content
187 (Zimmerman, 1971). The contribution of cosmic radiation to the total dose rate was calculated
188 as a function of latitude, altitude, burial depth and average over-burden density based on data
189 by Prescott and Hutton (1994). The OSL dates were then corrected with the average residual

age of the modern samples and confronted with the vertical floodplain aggradation, based on the relative vertical position of the samples above the Antalo limestone bedrock (in cm).

3. RESULTS

3.1 May Tsimble alluvial record

OSL age estimates (Table 3) are based on the concentration of radioisotopes within the sample and include corrections for cosmic radiation and moisture content (Appendix). Both the recent sample and the sample from the upper right terrace correspond to modern ages, which is consistent with the statements made by the interviewees. The other deposition dates range from 1846 ± 950 BCE to 1504 ± 290 CE. Despite the considerable errors due to the low sensitivity of the quartz, the dated sequence is consistent with the relative vertical position above the Antalo limestone bedrock. The dates point to a relatively simple genesis by floodplain aggradation instead of a more complex terrace genesis. One deposition date, sampled from the bottom of a profile pit, yielded a date of 22,976 ± 4760 BCE but this age estimate was strongly dependent upon the influence on the mean De estimate by a single outlier measurement. According to Wallinga (2002), the accuracy of OSL ages older than about 13 ka for such fluvial deposits can be dubious given the strong possibility of insufficient resetting at deposition and/or the inclusion of reworked older mineral grains having retained a residual signal (Duller, 2008). Because of this inconsistency this Pleistocene date was not considered.

TABLE 3

We corrected the luminescence ages for an average residual age of 300 years (200-400 years for samples X6432 and X6431), an order of magnitude that is in line with findings by Porat et

al. (2001). By confronting the dates with their vertical position above the bedrock, we calculated floodplain aggradation rates. We identify two broad periods of aggradation (Figure 4). A first period of aggradation is dated ~ 1500 BCE till 500 BCE, followed by a period of low aggradation rates from ~ 500 BCE till 500 CE. A second phase of high aggradation rates starts from ~ 500 CE onwards.

FIGURE 4

3.2 Wechi, Adwa and May Kinetal alluvial records

Based on three records of infilled valley deposits (the Wechi record, the Adwa record and the May Kinetal record) (Figure 5), Machado et al. (1998) identified three main stabilization periods over the past 4000 years (ca. 2000–1500 BCE, 500 BCE-500 CE and 950-1000 CE) with vertisol formation and three degradation episodes (ca. 1500–500 BCE, 500-950 CE, after 1000 CE) with increased sediment supply in Tigray. Because of the broad similarities with our record and the three records of Machado et al. (1998), we believe that the four records reflect a regional signal of altering geomorphic stability and degradation in the North Ethiopian Highlands. All the datasets confirm the occurrence of degradation periods during 1500-500 BCE and from 500 CE onwards. However, Machado et al. (1998) interpret these geomorphic degradation periods directly as phases of aridity, which should not necessarily be the case (Nyssen et al., 2004). Taking into account several independent high-quality paleoclimatic and palynological datasets obtained from lake cores in the region, a re-interpretation of these data is now proposed.

3.3 Correspondence with climate and land cover records

The paleoenvironmental records are schematized in Table 4 and localized on Figure 5. Broadly, we follow the evidence from stable carbon isotope and elemental analyses (Terwilliger et al., 2011), showing that human land clearings have had the dominant impact

237 on the Late-Holocene landscape in North Ethiopia as compared to climate changes. This is in
238 line with the view of Connah (2001), who states in his review on African civilizations that the
239 control of arable land and external trade are the two dominant factors determining this human
240 impact in the Horn of Africa, by mediating the emergence of elites and states.

241 We constructed a conceptual geomorphic model (Figure 6), under the reasonable assumption
242 that aggradation periods correspond with phases of increased sediment supply from slopes
243 into the valley, during phases of active degradation in the upper catchment. As a matter of
244 fact, in North Ethiopian ephemeral streams decreasing woody vegetation cover following land
245 clearings upstream leads to sediment accumulations downstream (Frankl et al., 2011). Indeed,
246 following the equations of Frankl et al. (2011), channel aggradation (d^-) results from an
247 increase in sediment supply (Q_s^+) (and/or a decrease in runoff Q^-). Simultaneously, channel
248 incision (d^+) follows an increase in water runoff (Q^+) and/or a decrease in sediment load (Q_s^-).
249 The earliest phase of incision might still be visible on historical photographs (late 19th
250 century) and a second incision phase is attributed to the late 20th century (Figure 6).

251 FIGURE 5

252 TABLE 4

253 FIGURE 6

254 *3.3.1 Geomorphic stability during the Cushitic era (before 1500 BCE)*

255 After the dry Younger Dryas and the dry Early Holocene, precession-driven insolation
256 changes initiated the African Humid Period (from 5650 BCE onwards) (Marshall et al., 2009).
257 We identified tufa deposits in the main May Tsimble channel on a waterfall next to our study
258 site (Figure 7b), possibly referring to the stable hydrogeomorphic conditions at that time
259 (Dramis et al., 2003; Moeyersons et al., 2006; Sagri et al., 2008). Pietsch and Machado (2012)

found evidence of soil formation under an open woodland cover during this period (near Yeha, Tigray). Later, there was a shift to Late Holocene dryer conditions at ~ 3650 BCE, perhaps already starting from ~ 4000 BCE (Marshall et al., 2009). However, at the same time, the *Podocarpus-Juniperus* forest in the Northern Highlands was still intact (Darbyshire et al., 2003). Mixed forest including *Podocarpus*, *Juniperus*, *Celtis* and *Olea* covered the landscape, somewhat similar to the present montane forest of central Ethiopia (Darbyshire et al., 2003). During the 3rd and 2nd millennium BCE (Late Bronze Age), paleosols indicate environmental stability (Pietsch and Machado, 2012). Overall, the geomorphic stability during this period seems independent from the Late-Holocene shift to dryer conditions (4000-3650 BCE; Marshall et al., 2009).

3.3.2 Aggradation during the Pre-Axumite chiefdoms (1500-500 BCE)

At the base of our sequence (Figure 7a), a first depositional unit was identified (Figure 4, lower part). It represents about 300 cm of aggradation, deposited between 1500-500 BCE, corresponding with the first degradation period of Machado et al. (1998). The onset corresponds to the start of deforestation determined by Moeyersons et al. (2006), who date backfill and overfill deposits of tufa dams in Tigray from 1430–1260 BCE onwards. Pietsch and Machado (2012) identify slope degradation and high sediment yield during the second half of the 2nd millennium. Similarly, Bard et al. (2000) report increased sedimentation at the Meskilo River (near Mekele) after the early second millennium BCE.

Despite the absence of significant climate changes during this period (Marshall et al., 2009), these dates do match or closely follow the introduction of cattle herding from Sudan in the North Ethiopian Highlands, at the beginning of the 2nd millennium BCE (Lesur et al., 2014). Indeed, the oldest evidence for domesticated cattle in North Ethiopia is dated to ~ 1800 BCE

(Marshall and Negash, 2002). Simultaneously, during the 2nd millennium BCE, chiefdoms rose in the Ethiopian Highlands and in the Gash (D'Andrea et al., 2008). 'Pre-Axumite chiefdoms' might be the best term to describe these social organizations because, despite the existence of the Sabaean ruins of Yeha, there was never a centralized 'Pre-Axumite state' (the so-called 'Damaat') (Phillipson, 2009). Pietsch and Machado (2012) identify decreased trees-to-shrub ratios over the Pre-Axumite times, as compared to the earlier Bronze Age.

More to the South (Lake Hayk), the timing of a rapid decline in *Podocarpus* and Cupressaceae forest is dated to 775–410 BCE (Darbyshire et al., 2003). At that time, the mixed conifer forest was replaced by disturbed, secondary bushland vegetation. Pollen evidence for this first large-scale deforestation concerns more than one taxon, indicating a dominant human interference, including vegetation clearance with the use of fire (Darbyshire et al., 2003). These large-scale deforestations happened about 600 years before deforestation in the Arsi and Bale Mountains (Hamilton, 1982), indicating a decreasing anthropogenic impact as one moves away from the Red Sea (Phillipson, 1985). Indeed, both the first deforestation and the high aggradation rates observed in May Tsimble by us, and in Wechi, Adwa and May Kinetal by Machado et al. (1998) coincide with migration of Semitic or Sabaean peoples from South Arabia towards Cushitic North Ethiopia, during the eighth and fifth century BC (Darbyshire et al., 2003).

3.3.3 Geomorphic stability during the (Proto-)Axumite state (500 BCE - 500 CE)

Much slower aggradation rates were dated between 500 BCE and 500 CE, although no clear discordance was observed in the profiles. Compared to the faster aggradation before 500 BCE, this period comprising 16 cm of aggradation must represent a phase of geomorphological stability. The phase corresponds with the soil formation period described

by Machado et al. (1998) (500 BCE-500 CE) and broadly coincides with the history of the Axumite state. French et al. (2009) indeed infer considerable landscape stability both during and prior to the Aksumite Period, evidenced by the development of vertic-like soils. In *The History*, Herodotos of Halicarnassos (430 BCE) describes Ethiopia as a very rich civilization. Following an explosion of demand for South Indian products in the Roman Empire (Rome, later Byzantium), there was a strong expansion of the Indian Ocean trade through the Red Sea, giving rise to the urban Axum Empire (Burstein, 2001; Phillipson, 2012). As reported in the *Periplus of the Erythraean Sea,* Adulis was an important sea port. The hegemony over the Red Sea and the Upper Nile ensured trade with Persians, Nubians and Yemen, while achieving the monopoly over trade routes to central Africa (D'Andrea et al., 2008). It can be assumed that increased resources allowed reducing pressure on the lands, as Bard et al. (2000) claim that no reduction in soil productivity can be found over the Axumite era. Pietsch and Machado (2012) identify increased trees-to-shrub ratios over the Axumite times, as compared to the Pre-Axumite period. Following Ciampalini et al. (2008), there are the Proto-Axumite (from ~ 450 BCE), Early Axumite (from ~ 90 BCE) and Classic Axumite (from ~ 100 CE) eras. Erosion rates in the immediate surroundings of Axum, calculated for these three main intervals are relatively low, proving the strong positive impact of Axum's extensive soil and water conservation (dams and terraces) (Ciampalini et al., 2008) and long-term landscape management by the growing population (French et al., 2009). However, this was a relatively dry period in the Highlands (Lamb et al., 2007). Generally, it is recognized that adoption and intensity of investments in water and soil conservation are positively dependent on land tenure security and farmers income (Kabubo-Mariara et al., 2006). During periods of social security, agricultural technology and intensification prosper while long-term conservation issues prevail over short-term survival (Nyssen et al., 2004). The impact of climate changes remains

unclear but Marshall et al. (2009) suggest increased wetness in northern Ethiopia between 350 BCE and 450 CE.

3.3.4 Aggradation during the Post-Axumite era (500-1000 CE)

A second phase of faster aggradation rates was dated from 500 CE onwards, when more than 150 cm of sediment vertically filled the valley bottom. Since we did not measure sediment volumes, the vertical aggradation depth only gives an indication of the amount of deposited sediment – volumetric increase rate is assumed to be many times more important, given the triangular shape of the infilled valley bottom. Again, the ages correspond well with the degradation period (500-1000 CE) identified by Machado et al. (1998). At Lake Ashenge, pollen evidence points to an abrupt *Podocarpus* decline and enhanced soil erosion by 500 CE, under intensified land use (Marshall et al., 2009). Arab expansions from the 6th century onwards excluded Axum from the Indian Ocean trade system, leading to the chaotically post-Axumite era. Population continued to grow (McEvedy and Jones, 1978), deforestation progressed from 900 CE onwards (Darbyshire et al., 2003) and around 800 CE 'roving kingdoms' were rivaling over the Ethiopian plateau (Abebe, 1998) while famines and plagues culminated between 831-849 CE (Bard et al., 2000). The onset of this second aggradation period could coincide with a shift to a dryer climate around 500 CE (Marshall et al., 2009), but this shift was not identified at Lake Hayk and soon a wet period followed (700-750 CE) (Lamb et al., 2007), possibly lasting till 950 CE (Marshall et al., 2009).

3.3.5 Possible geomorphic stability under the Zagwe state (1000-1150 CE)

Machado et al. (1998) identified another period of low sediment activity (calibrated dates from 1013-1164 CE), which could have been left undetected in the May Tsimble record given its lower resolution. Brancaccio et al. (1997) also report on pedogenesis around 700 and 980

CE. This Medieval Warm Period (750-1200 CE) is in North Ethiopia relatively dry (Lamb et al., 2008). However, the centralized Zagwe rule (1000-1250 CE) based in the Lasta region, was rather peaceful, stable and urban and was involved in long-distance trade from the port of Zayla (Pankhurst, 1997; Tekeste Negash, 2006). More datasets are required to investigate the specificities of human-environment interactions at that time.

3.3.6 Aggradation during the 'Early Medieval Times'

A third phase of faster aggradation rates was reported by Machado et al. (1998) after 1050 CE. As the stabilization phase discussed above (~ 1000-1050 AD) was undetected in the May Tsimble record, these faster aggradation rates are there dated from 500 CE onwards. However, the 'Little Ice Age' was quite wet in North Ethiopia, characterized by another wet interval around 1300 CE and a small drought around 1550 CE (Lamb et al., 2007). By contrast, following intensification of grazing, grasslands were expanding around 1200-1400 CE (Darbyshire et al., 2003). European historical sources from the 'Early Medieval times' report on vast amounts of cattle and grasslands under large-scale deforestation in Ethiopia (Pankhurst, 1990). There were frequent civil wars with rebelling vassals or Muslim lowlanders during this unstable Solomonic dynasty. Lands were owned by noblemen or by the Church while reported in *Il Milione* by Marco Polo (from second hand information), trade was dominated by Arabs (and some Armenians). Instead of a fixed capital, there were 'moving camps', and there are many reports on crop plagues by locusts and rats (Pankhurst, 1990).

3.3.7 Late Medieval reforestation

During the 'Late Medieval times', Darbyshire et al. (2003) identified a gradual reforestation of *Juniperus*-dominated dry Afromontane forest between 1400 and 1700 CE. Following the war between the Adal Sultanate and Ethiopia and Portugal, Oromo peoples moved to the

Highlands and their nomadic pastoralism reduced pressure on the land (Darbyshire et al., 2003). Portuguese reports state fewer cattle in the early 16th (Thomas of Angot) and 17th century (Manuel de Almeida) (Pankhurst, 1990). Under the new capital of Gondar (1632) and commercialization of agriculture, the late 17th century was an urban period of renaissance, trading with Sudan and from the port of Massawa (Pankhurst, 1990). The rise of Gondar occurred despite a drying trend since 1650 CE (Lamb et al., 2007). Little information on geomorphic activity is available for this period, although a phase of soil formation has been dated up to 1641 AD in Adi Kolen (Bard et al., 2000). It must be noted that such periods of soil formation can also result from a particular local evolution of vegetation cover (Nyssen et al., 2004), so again more data must be gathered to identify spatial-regional patterns. Also note the possibility that the stabilized channel incisions that are visible on 19th-century terrestrial photographs (see Frankl et al., 2011) result from a *clear water effect* under an increased Late Medieval vegetation cover.

3.3.8 The 20th century

Finally, according to the semi-structured interviews with farmers around our study site, the May Tsimble stream incised and shifted its channel to the right (i.e. to the West) around the 1960s-1970s. Gully incision has been observed at regional scale during this period (Frankl et al., 2011, 2013). In the modern channel, very recent re-incision is visible as a small intra-channel terrace. It might be the result of a clear-water effect after the large-scale implementation of conservation measures (including the dam pictured in Fig. 3), following increased sediment supply during the 1960s-1980s. These phases correspond well with the three main geomorphic periods over the 20th century identified by Lanckriet et al. (2014b) and Frankl et al. (2011). There is the *feudal era*, with some widely implemented conservation structures (such as *dagets*) (Lanckriet et al., 2014b), quite stable channels with an oversized

inherited morphology and low sediment supply (Frankl et al., 2010). Following strongly increased runoff coefficients, a general incision phase was documented to start in the (late feudal) 1960s. It continued through the civil war as strengthened by the effect of droughts and a lack on investments in conservation during the 1980s (Frankl et al., 2011). Finally, there is the *post-war era*, with new conservation efforts, more equal land rights (Lanckriet et al., 2014b) and again lower sediment supply and lower runoff response (Frankl et al., 2011).

FIGURE 7

4. DISCUSSION

Periods of stronger geomorphic activity do not directly coincide with periods of increased aridity; although this does not strictly imply that more indirect or nonlinear climate-land interactions did not occur.

Geomorphic stability is for instance present under both dry and wet conditions. Low geomorphic activity before 1500 BCE is not in phase with the much earlier shift to dryer conditions (3650 BCE; Marshall et al., 2009). The same is true for the first wave of large-scale deforestation during the second-first millennium BCE (Darbyshire et al., 2003). Geomorphic stability matching the emergence of the (Proto-)Axumite state (broadly from 500 BCE to 500 CE) (French et al., 2009) occurred during a relatively dry period (Lamb et al., 2007). Note that the diatom evidence from the Lake Ashenge record suggesting increased wetness between 200 BCE - 500 CE is not evidenced by stable isotopes (Marshall et al., 2009). A period of lower sediment supply dated to 1013-1164 CE (Machado et al., 1998) happened during the relatively dry Medieval Warm Period (Lamb et al., 2007) while relatively high geomorphic activity in the Highlands from 1050 to 1700 CE coincides with the wetter Little Ice Age.

Land cover records further indicate three waves of deforestation and subsequent reforestation in the Highlands, suggesting but not clearly exhibiting a link with dry or wet periods. A *Podocarpus-Juniperus* forest dominated the Highlands before the first millennium BCE, while the earliest pollen evidence for forest decline in the Ethiopian Highlands was linked with Semitic immigrations instead of drought (Darbyshire et al., 2003). Thereafter scrub and grassland vegetation persisted for about 1800 years; with a specific dominance of grasslands from ~ 1200 to 1400 CE (Darbyshire et al., 2003). Despite the dominance of scrub and grassland vegetation from 500 BCE to 500 CE, the landscape was relatively stable (French et al., 2009). Forest regrowth then did occur during the wet Little Ice Age as *Juniperus*, *Olea* and *Celtis* forest extent increased again from 1400 to 1700 CE (Darbyshire et al., 2003; Lanckriet et al., 2015). The second phase of large-scale deforestation during the dry 18th century was evidenced from pollen analysis by Darbyshire et al. (2003) and by Lanckriet et al. (2015), who identified an 18th century decline in *Olea*, *Celtis* and *Podocarpus* under an increase in Poaceae pollen. Consequently, the Northern Ethiopian Highlands were heavily deforested in the 19th century (Nyssen et al., 2009) when already considerable runoff was produced (Lanckriet et al., 2014a). A minimal woody vegetation cover persisted from the 1950s to the 1990s (Lanckriet et al., 2015), overlapping with the dry decade of the 1980s, but a new period of increased forest extent is evident over the last two decades (Nyssen et al., 2014). Nyssen et al. (2009) hence show that nowadays, instead of total degradation, an increase of woody biomass can be observed.

Finally it is worth mentioning that long-term and extreme dry conditions in the Highlands are a relatively rare phenomenon. The isotope record from Lake Hayk shows that the regional climate during the last two millennia was generally always moister than at present, with only two exceptions (a phase around 800 CE and from 1750 to 1880 CE) (Lamb et al., 2007).

5. CONCLUSIONS

In this study, we reviewed a number of paleo environmental records from the North Ethiopian Highlands and additionally used optically stimulated luminescence to date aggradation phases in the May Tsimble catchment (North Ethiopia). Preceded and interrupted by periods of low aggradation rates, we identified two periods of faster alluvial deposition in the catchment, from 1500-500 CE and after 500 CE. The results are consistent with radiocarbon dating results from the Wechi, Adwa and May Kinetal catchments. We infer that the sequence of terraces in May Tsimble is resulting from two depositional phases, followed by recent incision. Stable channels observable on mid-19th-century terrestrial photographs indicate at least one earlier incision phase. Comparison with independent records from lake sediments shows that periods of faster aggradation do not correspond directly with periods of increased aridity or wetness. There is however a clear dominant human impact, as the first degradation phase coincides with the introduction of cattle herding and the second phase with the post-Axumite era. The Late-Holocene history of geomorphic activity in the Ethiopian Highlands, often interpreted as directly driven by climate, bears imprints of investments in soil and water conservation during periods of social chaos.

Acknowledgements:

This study would not have been possible without the enormous support, friendship and help of our translator Gebrekidan Mesfin, the important input on mineralogy from Florias Mees, the advice from Dimitri Vandenberghe, the support and kindliness of the farmers near the study site, the kind hospitality of the Luminescence Dating Laboratory of the University of Oxford, the funding of UGent Special Research Fund, as well as the logistical support through Belgian VLIR projects at Mekelle University (IUC and Graben TEAM).

6. REFERENCES

Abebe, B., 1998. Histoire de L'Éthiopie d'Axoum à la revolution. Maisonneuve et Larose, Paris.

Aitken, M.J., 1985. Thermoluminescence Dating. Academic Press, New York.

Adamiec, G., Aitken, M.J., 1998. Dose-rate conversion factors: new data. Ancient TL. 16, 37-50.

Alexanderson, H., 2007. Residual OSL signals from modern Greenlandic river sediments. Geochronometria 26, 1-9.

Arnold, L., Bailey, R., Tucker, G., 2007. Statistical treatment of fluvial dose distributions from southern Colorado arroyo deposits. Quaternary Geochronology 2, 162-167.

Arnold, L., Roberts, R., Galbraith, R., DeLong, S., 2009. A revised burial dose estimation procedure for optical dating of young and modern-age sediments. Quaternary Geochronology 4, 306-325.

Avni, Y., Porat, N., Plakht, J., Avni, G., 2006. Geomorphic changes leading to natural desertification versus anthropogenic land conservation in an and environment, the Negev Highlands, Israel. Geomorphology 82 (3-4), 177-200.

Avni, Y., Zhang, J., Shelach, G., Zhou, L., 2010. Upper Pleistocene-Holocene geomorphic changes dictating sedimentation rates and historical land use in the valley system of the Chifeng region, Inner Mongolia, northern China. Earth Surface Processes and Landforms 35 (11), 1251-1268.

Avni, Y., Porat, N., Avni, G., 2012. Pre-farming environment and OSL chronology in the Negev Highlands, Israel. Journal of Arid Environments 86, 12-27.

Bailey, R., Arnold, L., 2006. Statistical modelling of single grain quartz D-e distributions and an assessment of procedures for estimating burial dose. Quaternary Science Reviews 25 (19-20), 2475-2502.

Banerjee, D, Murray, A S, Bøtter-Jensen, L, Lang, A., 2001. Equivalent dose estimation using a single aliquot of polymineral fine grains, Radiation Measurements 33, 73-94.

Bard K., Coltorti, M., Di Blasi, M., Dramis F., Fattovich, R., 2000. The environmental history of Tigray (Northern Ethiopia) in the Middle and Late Holocene: a preliminary outline. African Archaeological Review 17 (2), 65-86.

Botha, G., Wintle, A., Vogel, J., 1994. Episodic Late Quaternary palaeogully erosion in Northern Kwazulu Natal, South Africa. Catena 23 (3-4), 327-340.

Bøtter-Jensen, L., 1988. The automated Risø TL dating reader system. Nuclear Tracks and Radiation Measurements 14, 177–180.

Bøtter-Jensen, L., 1997. Luminescence techniques: instrumentation and methods. Radiation Measurements 27, 749–768.

Bøtter-Jensen, L., Bulur, E., Duller, G.A.T., Murray, A.S., 2000. Advances in luminescence instrument systems. Radiation Measurements 32, 523–528.

Bourke, M., Child, A., Stokes, S., 2003. Optical age estimates for hyper-arid fluvial deposits at Homeb, Namibia. Quaternary Science Reviews 22, 1099–1103.

Brancaccio, L., Calderoni, G., Coltorti, M., Dramis, F., 1997. Phases of soil erosion during the Holocene in the Highlands of Western Tigray (Northern Ethiopia): a preliminary report.

In: Bard, K. (Ed.), The Environmental History and Human Ecology of Northern Ethiopia in the Late Holocene. Instituto Universitario Orientale, Napoli, pp. 30 – 48.

Broothaerts, N., Verstraeten, G., Notebaert, B., Assendelft, R., Kasse, C., Bohncke, S., Vandenberghe, J., 2013. Sensitivity of floodplain geoecology to human impact: A Holocene perspective for the headwaters of the Dijle catchment, central Belgium. The Holocene 23 (10), 1403-1414.

Burstein, S., 2001. State formation in ancient Northeast Africa and the Indian Ocean Trade. Conference Proceeding of the American Historical Association: Interactions, Regional Studies, Global Processes, and Historical Analysis: 28 February 2001, Library of Congress, Washington D.C. Accessed on 02 December 2014 and available from: http://webdoc.sub.gwdg.de/ebook/p/2005/history_cooperative/www.historycooperative.org/proceedings/interactions/burstein.html

Bussert, R., Schrank, E., 2007. Palynological evidences for a latest Carboniferous-Early Permian glaciation in Northern Ethiopia. Journal of African Earth Science 49, 201-210.

Carnicelli, S., Benvenuti, M., Ferrari, G., Sagri, M., 2009. Dynamics and driving factors of late Holocene gullying in the Main Ethiopian Rift (MER). Geomorphology 103 (2), 541-554.

Chen, J., Dai, F., Yao, X., 2008. Holocene debris-flow deposits and their implications on the climate in the upper Jinsha River valley, China. Geomorphology 93 (3-4), 493-500.

Ciampalini, R., Billi, P., Ferrari, G., Borselli, L., 2008. Plough marks as a tool to assess soil erosion rates: A case study in Axum (Ethiopia). Catena 75, 18–27.

Collins, R., 1999. Macrohistory: Essays in Sociology of the Long Run. Stanford University Press, Redwood City, USA, 312 p.

546 Connah, G., 2001. African Civilizations: An Archaeological Perspective. Cambridge
547 University Press, 340 p.

548 Costas, I., Reimann, T., Tsukamoto, S., Ludwig, J., Lindhorst, S., Frechen, M., Hass, H.,
549 Betzler, C., 2012. Comparison of OSL ages from young dune sediments with a high-
550 resolution independent age model. Quaternary Geochronology 10, 16–23.

551 D'Andrea, C., Manzo, A., Harrower, M., Hawkins, A., 2008. The Pre-Aksumite and
552 Aksumite Settlement of NE Tigrai, Ethiopia. Journal of Field Archaeology 33, 151-176.

553 Darbyshire, I., Lamb, H., Umer, M., 2003. Forest clearance and regrowth in northern Ethiopia
554 during the last 3000 years. The Holocene 13, 537–546.

555 Dramis, F., Umer M., Calderoni G., Haile M., 2003. Holocene climate phases from buried
556 soils in Tigray (northern Ethiopia): Comparison with lake level fluctuations in the Main
557 Ethiopian Rift. Quaternary Research 60, 274-283.

558 Duller, G., 2008. Luminescence dating: guidelines on using luminescence dating in
559 archaeology. Swindon: English Heritage.

560 Eipert, A., 2004. Optically stimulated luminescence (OSL) dating of sand deposited by the
561 1960 tsunami in south-central Chile, Geology Comps Papers.

562 Eriksson, M., Olley, J., Payton, R., 2000. Soil erosion history in central Tanzania based on
563 OSL dating of colluvial and alluvial hillslope deposits. Geomorphology 36 (1-2), 107-128.

564 Frankl, A., Nyssen, J., De Dapper, M., Haile, M., Billi, P., Munro, N., Deckers, J., Poesen, J.,
565 2011. Linking long-term gully and river channel dynamics to environmental change using
566 repeat photography (Northern Ethiopia). Geomorphology 129, 238-251.

567 Frankl, A., Poesen, J., Scholiers, N., Jacob, M., Haile Mitiku, Deckers, J., Nyssen, J., 2013.
568 Factors controlling the morphology and volume (V) – length (L) relations of permanent
569 gullies in the Northern Ethiopian Highlands. Earth Surf. Process. Landforms 38, 1672-1684.

570 French, C., Sulas, F., Madella, M., 2009. New geoarchaeological investigations of the valley
571 systems in the Aksum area of northern Ethiopia. Catena 78 (3), 218–233.

572 Galbraith, R., Roberts, R., Laslett, G., Yoshida, H., 1999. Optical dating of single and
573 multiple grains of quartz from Jinmium rock shelter, Northern Australia: Part I, experimental
574 design and statistical models. Archaeometry 41 (2), 339–364.

575 Goudie, A., 2013. The Human Impact on the Natural Environment: Past, Present, and Future.
576 John Wiley and Sons, Hoboken, New Jersey.

577 Hamilton, A., 1982. Environmental history of East Africa. London: Academic Press, 328 pp.

578 Harvey, J., Pederson, J., Rittenour, T., 2011. Exploring relations between arroyo cycles and
579 canyon paleoflood records in Buckskin Wash, Utah: Reconciling scientific paradigms.
580 Geological Society of America Bulletin 123 (11-12), 2266-2276.

581 Herodotos of Halicarnassos, 430 BCE, The Histories: Muse 3, 114.1. In: The History, trans.
582 George Rawlinson, New York: Dutton, 1862.

583 Kabubo-Mariara, J., Linderhof, V., Kruseman, G., Atieno, R., Mwabu, G., 2006. Household
584 Welfare, Investment in Soil and Water Conservation and Tenure Security: Evidence From
585 Kenya. PREM Working Paper: PREM 06/06.

586 Keen-Zebert, A., Tooth, S., Rodnight, H., Duller, G., Roberts, H., Grenfell, M., 2013. Late
587 Quaternary floodplain reworking and the preservation of alluvial sedimentary archives in

588 unconfined and confined river valleys in the eastern interior of South Africa. Geomorphology
589 185, 54-66.

590 Lamb, H., Leng, M., Telford, R., Tenalem Ayenew, Umer, M., 2007. Oxygen and carbon
591 isotope composition of authigenic carbonate from an Ethiopian lake: a climate record of the
592 last 2000 years. The Holocene 17(4), 517–526.

593 Lanckriet, S., Frankl, A., Descheemaeker, K., Gebrekidan Mesfin, Nyssen, J., 2014a. Gully
594 cut-and-fill cycles as related to agro-management: a historical curve number simulation in the
595 Tigray Highlands. Earth Surface Processes and Landforms: in press.

596 Lanckriet, S., Derudder, B., Naudts, J., Tesfay Araya, Cornelis, W., Bauer, H., Deckers, J.,
597 Mitiku Haile, Nyssen, J., 2014b. A political ecology perspective of land degradation in the
598 North Ethiopian Highlands. Land Degradation and Development, online early view.

599 Lanckriet, S., Frankl, A., Enyew Adgo, Termonia, P., Nyssen, J., 2014c. Droughts related to
600 quasi-global oscillations: a diagnostic teleconnection analysis in North Ethiopia. International
601 Journal of Climatology, in press.

602 Lanckriet, S., Rucina, S., Frankl, A., Ritler, A., Gelorini, V., Nyssen, J., 2015. Nonlinear
603 vegetation cover changes in the North Ethiopian Highlands: evidence from the Lake Ashenge
604 closed basin. Science of the Total Environment: submitted.

605 Lang, A., Mauz, B., 2006. Towards chronologies of gully formation: optical dating of gully
606 fill sediments from Central Europe. Quaternary Science Reviews 25 (19-20), 2666-2675.

607 Lehmkuhl, F., Hilgers, A., Fries, S., Hulle, D., Schlutz, F., Shumilovskikh, L., Felauer, T.,
608 Protze, J., 2011. Holocene geomorphological processes and soil development as indicator for
609 environmental change around Karakorum, Upper Orkhon Valley (Central Mongolia). Catena
610 87 (1), 31-44.

611 Leigh, D.S., Kowalewski, S.A., Holdridge, G.H., 2013. 3400 Years of Agricultural
612 Engineering in Mesoamerica: Lama-Bordos of the Mixteca Alta, Oaxaca, Mexico. Journal of
613 Archaeological Science 40, 4107-4111.

614 Lesur, J., Hildebrand, E., Abawa, G., Gutherz, X., 2014. The advent of herding in the Horn of
615 Africa: New data from Ethiopia, Djibouti and Somaliland. Quaternary International, in press.

616 Machado, M., Pérez-González, A., Benito, G., 1998: Paleoenvironmental changes during the
617 last 4000 yr in the Tigray, Northern Ethiopia. Quaternary Research 49, 312–21.

618 Marshall, F., Negash, A., 2002. Early hunters and herders of northern Ethiopia: The fauna
619 from Danei Kawlos and Baati Ataro rockshelters. Society for African Archaeologists
620 Meeting. Tucson, Arizona.

621 Marshall, M., Lamb, H., Davies, S., Leng, M., Zelalem Kubsa, Umer, M., Bryant, C., 2009.
622 Climatic change in northern Ethiopia during the past 17,000 years: A diatom and stable
623 isotope record from Lake Ashenge. Palaeogeography, Palaeoclimatology, Palaeoecology 279,
624 114–127.

625 McCann, J., 1997. The Plow and the Forest: Narratives of Deforestation in Ethiopia 1840-
626 1992. Environmental History 2 (2), 138-159.

627 McEvedy, C., Jones, R., 1978. Atlas of World Population History (Hist Atlas). Puffin,
628 London, UK, 368 p.

629 Mejdahl, V., 1979. Thermoluminescence dating: beta-dose attenuation in quartz grains.
630 Archaeometry. 21, 61-72.

631 Merla, G., Abbate, E., Azzaroli, A., Bruni, P., Canuti, P., Fazzuoli, M., Sagri, M. Tacconi, P.,
632 1979. A Geological Map of Ethiopia and Somalia (1973). 1 : 2 000 000; and Comment.
633 University of Florence, Firenze.

634 Moeyersons, J., Nyssen, J., Poesen, J., Deckers, J., Mitiku Haile, 2006. Age and
635 backfill/overfill stratigraphy of two tufa dams, Tigray Highlands, Ethiopia: Evidence for Late
636 Pleistocene and Holocene wet conditions. Palaeogeography, Palaeoclimatology,
637 Palaeoecology 230 (1–2), 165–181.

638 Murray, A.S., Wintle, A.G., 2000. Luminescence dating of quartz using an improved single-
639 aliquot regenerative-dose protocol. Radiation Measurements 32, 57-73.

640 Nicholson, S., Dezfuli, A., Klotter, D., 2012. A two-century precipitation dataset for the
641 continent of Africa. American Meteorological Society. DOI:10.1175/BAMS-D-11-00212.1.

642 Nyssen, J., Poesen, J., Moeyersons, J., Deckers, J., Mitiku Haile, Lang, A., 2004. Human
643 impact on the environment in the Ethiopian and Eritrean highlands--a state of the art. Earth-
644 Science Reviews 64 (3-4), 273-320.

645 Nyssen, J., Poesen J., Veyret-Picot, M., Moeyersons, J., Mitiku Haile, Deckers, J., Dewit, J.,
646 Naudts, J., Teka, K., Govers, G., 2006. Assessment of gully erosion rates through interviews
647 and measurements: a case study from northern Ethiopia. Earth Surface Processes and
648 Landforms 31 (2), 167–185.

649 Nyssen, J., Haile, M., Naudts, J., Munro, N., Poesen, J., Moeyersons, J., Frankl, A., Deckers,
650 J., Pankhurst, R., 2009. Desertification? Northern Ethiopia re-photographed after 140 years.
651 Sci Total Environ 407, 2749–2755.

652 Nyssen, J., Frankl, A., Mitiku Haile, Hurni, H., Descheemaeker, K., Crummey, D., Ritler, A.,
653 Portner, B., Nievergelt, B., Moeyersons, J., Munro, R.N., Deckers, J., Billi, P., Poesen, J.,

2014. Environmental conditions and human drivers for changes to north Ethiopian mountain landscapes over 145 years. Science of the Total Environment, in press.

Pankhurst, R., 1990. A Social History of Ethiopia: The Northern and Central Highlands from Early Medieval Times to the Rise of Emperor Tewodros II. Addis Ababa University, 371 pp.

Pankhurst, R., 1997. The Ethiopian Borderlands: Essays in Regional History from Ancient Times to the end of the 18th century. The Red Sea Press: Asmara, Eritrea.

Pelletier, J., Quade, J., Goble, R., Aldenderfer, M., 2011. Widespread hillslope gullying on the southeastern Tibetan Plateau: Human or climate-change induced? Geological Society of America Bulletin 123 (9-10), 1926-1938.

Phillipson, D. 1985. African archaeology. Cambridge: Cambridge University Press, 234 pp.

Phillipson, D., 2009. The First Millennium BC in the Highlands of Northern Ethiopia and South–Central Eritrea: A Reassessment of Cultural and Political Development". African Archaeological Review 26, 257–274.

Phillipson, D., 2012. Aksum and the Northern Horn of Africa. Archaeology International 15, 49-52.

Pietsch, D., Machado, M., 2012. Colluvial deposits – proxies for climate change and cultural chronology. A case study from Tigray, Ethiopia. Zeitschrift für Geomorphologie, Supplementary Issues 58, 119-136.

Poesen, J., Vandekerckhove, L., Nachtergaele, J., Oostwoud Wijdenes, D., Verstraeten, G., van Wesemael, B., 2002. Gully erosion in dryland environments. In: Bull, L.J., Kirkby, M.J. (Eds.), Dryland Rivers: Hydrology and Geomorphology of Semi-Arid Channels. Wiley, Chichester, UK, pp. 229–262.

676 Porat, N., Zilberman, E., Amit, R., Enzel, Y., 2001. Residual ages of modern sediments in an
677 hyperarid region, Israel. Quaternary Science Reviews 20 (5-9), 795-798.

678 Prescott, J. R., Hutton, J. T., 1994. Cosmic ray contributions to dose rates for luminescence
679 and ESR dating: large depths and long-term time variations. Radiation Measurements 23,
680 497–500.

681 Sagri, M., Bartolini, C., Billi, P., Ferrari, G., Benvenuti, M., Carnicelli, S., Barbano, F., 2008.
682 Latest Pleistocene and Holocene river network evolution in the Ethiopian Lakes Region.
683 Geomorphology 94, 79–97.

684 Schoff, W., 1912. The Periplus of the Erythraean Sea - Periplus maris Erythraei (English
685 translation), New York: Longmans, Green.

686 Schütt, B., Frechen, M., Hoelzmann, P., Fritzenwenger, G., 2011. Late Quaternary landscape
687 evolution in a small catchment on the Chinese Loess Plateau. Quaternary International 234,
688 159-166.

689 Shaw, A., Holmes, P., Rogers, J., 2001. Depositional landforms and environmental change in
690 the headward vicinity of Dias Beach, Cape Point. South African Journal of Geology 101 (2),
691 101-114.

692 Summa-Nelson, M., Rittenour, T., 2012. Application of OSL dating to middle to late
693 Holocene arroyo sediments in Kanab Creek, southern Utah, USA. Quaternary Geochronology
694 10, 167-174.

695 Teeuw, R., Rhodes, E., Perkins, N., 1999. Dating of quaternary sediments from western
696 Borneo, using optically stimulated luminescence. Singapore Journal of Tropical Geography
697 20 (2), 181-192.

698 Tekeste Negash, 2006. The Zagwe period re-interpreted: post-Aksumite Ethiopian urban
699 culture. Africa: Rivista Trimestrale di Studi e Documentazione 61 (1), 120-137.

700 Terwilliger, V.J., Eshetu, Z., Huang,Y., Alexandre,M., Umer, M. and Gebru,T., 2011. Local
701 variation in climate and land use during the time of the major kingdoms of the Tigray Plateau
702 in Ethiopia and Eritrea. Catena 85, 130–143.

703 Thomas, M., Murray, A., 2001. On the age and significance of Quaternary colluvium in
704 eastern Zambia. Palaeoecology of Africa and the surrounding islands 27, 117-133.

705 Tooth, S., Hancox, P., Brandt, D., McCarthy, T., Jacobs, Z., Woodborne, S., 2013. Controls
706 On the Genesis, Sedimentary Architecture, and Preservation Potential of Dryland Alluvial
707 Successions In Stable Continental Interiors: Insights from the Incising Modder River, South
708 Africa. Journal of sedimentary research 83 (7-8), 541 -561.

709 Vanmaercke M, Poesen J, Verstraeten G, Maetens W, de Vente J., 2011. Sediment yield as a
710 desertification risk indicator. Science of the Total Environment 409, 1715-1725.

711 Vanmaercke, M., Poesen, J., Broeckx, J., Nyssen, J., 2014. Sediment Yield in Africa. Earth-
712 Science Reviews 136, 350-368.

713 Wallinga, J., 2002. Optically stimulated luminescence dating of fluvial deposits: a review.
714 Boreas 31 (4), 303-322.

715

716 Wintle, A.G. and Murray, A.S., 2006. A review of quartz optically stimulated luminescence
717 characteristics and their relevance in single-aliquot regeneration dating protocols. Radiation
718 Measurements 41, 369-391.

719 Zimmerman, D.W., 1971. Thermoluminescent dating using fine grains from pottery.
720 Archaeometry 13, 29-50.

721

722

723

FIGURES

See separate file

726 TABLES

727 Table 1. Luminescence dating of ephemeral stream deposits all over the world. Only relevant
728 papers (empirical research on Late Pleistocene or Holocene stream deposits) were
729 incorporated in the review. Note that OD = Over Dispersion; IRSL = Infra-Red Stimulated
730 Luminescence; and MAM = Minimum Age Model.

731

732 *See separate document*

733

734 Table 2: Geology and mineralogy of the four catchments investigated during the
735 reconnaissance survey.

Location	Sampled location (WGS84)	Geology of the catchment	Mineralogy of the sandy fraction (250-106µm) in the sampled fill sediments
May Mekden	13.57834 °N, 39.57178 °E	Agula shales and Antalo limestone	90 % micritic limestone fragments; 10 % quartz; some zircon, sparitic calcite grains
Nebelet	14.12790 °N, 39.26888 °E	Enticho sandstone cliffs with underlying Precambrian metavolcanics	Nearly exclusively quartz; some opaque grains; mudstone fragments; possible plagioclase and microcline
May Tsimble	13.40372 °N, 39.67131°E	Antalo limestone with dolerite and sandstone near the water divide	Nearly exclusively quartz; some plagioclase and microcline; opaque grains

Ashenge	12.56571 °N, 39.51157 °E	Tertiary basalts (Ashangi group) and consolidated volcanic ashes	70 % hornblende; 25 % opaque grains; 5 % plagioclase; some quartz, zircon, biotite, muscovite

736

737

738 FIGURES

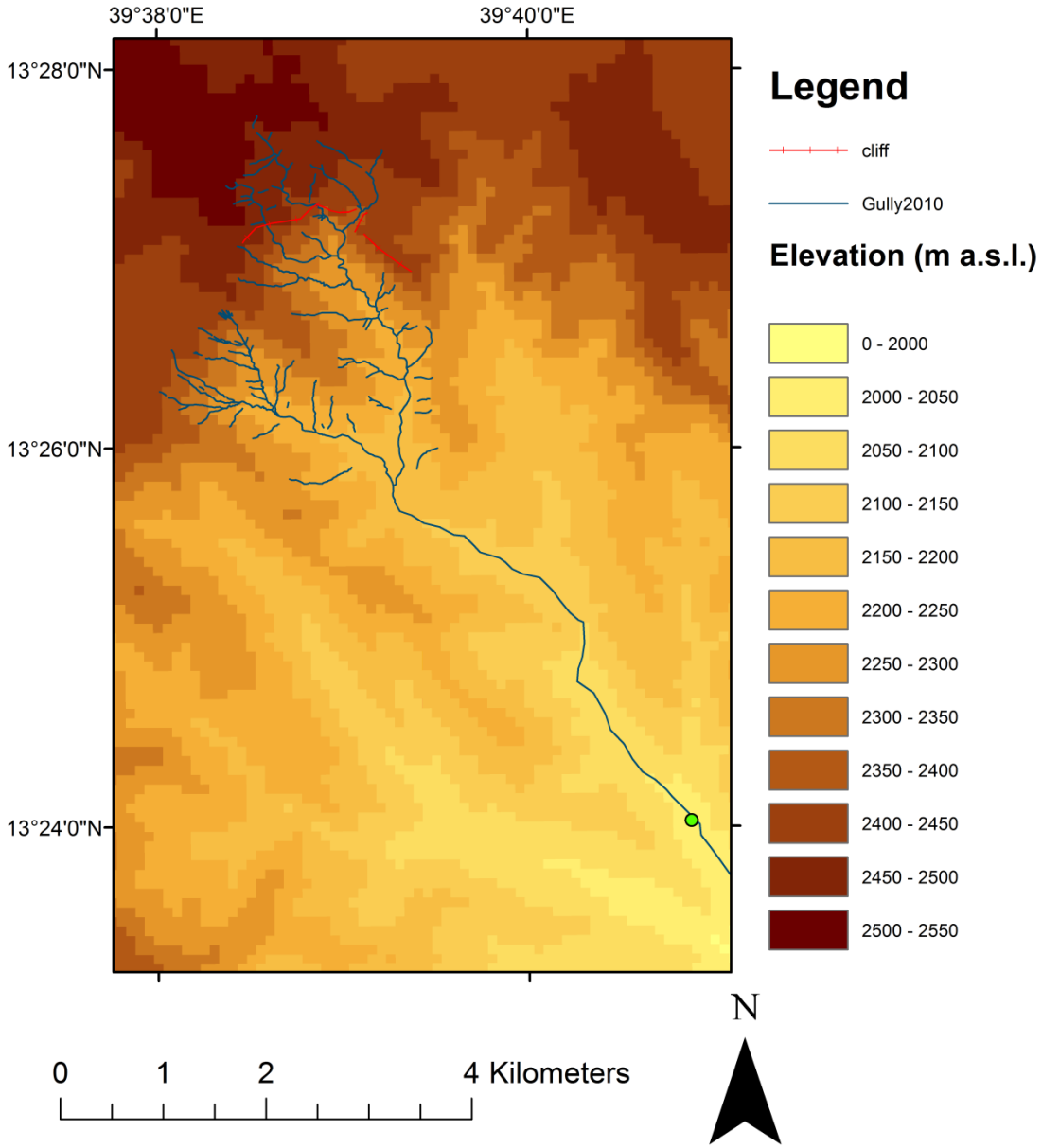

739

740 Figure 1. Upper stream network in the May Tsimble catchment, upstream of our sampling site
741 (indicated with green dot). For general localization of the catchment, see Figure 5 (location
742 C).

743

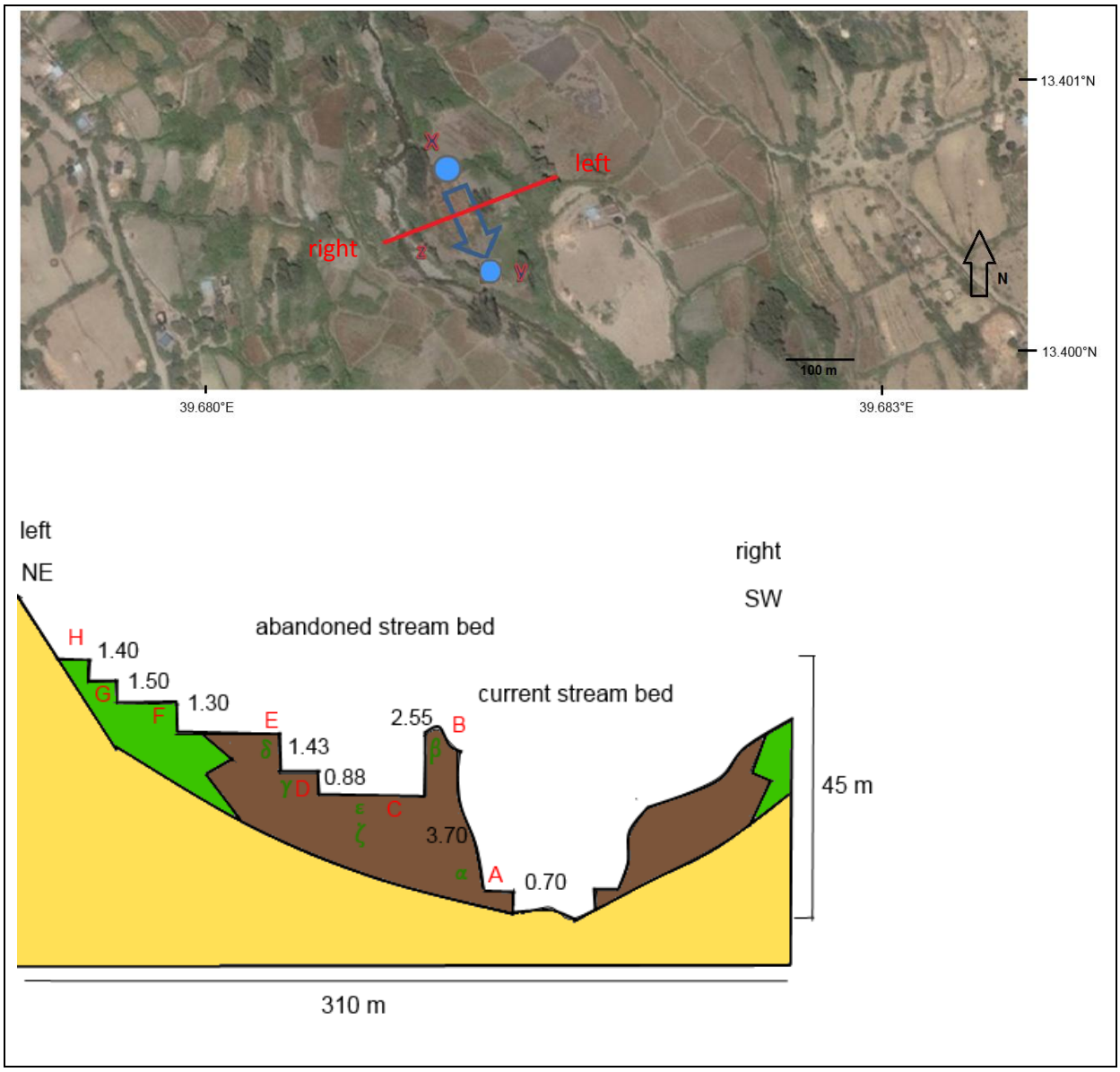

Figure 2. Location of the study site from a BingMaps® satellite image with blue dots indicating the start and end of the paleo channel and the blue arrow indicating the paleo stream direction (up); and schematic profile of the study site with sequence of terraces (below) as indicated on the satellite image by red line, including relative heights (in m), coded terraces or locations (in red Latin letters) and OSL sample field codes (in green Greek letters). The Antalo limestone bedrock is indicated in yellow, colluvium in green and alluvium is indicated in brown. The inlet of the paleochannel (13.40114°N; 39.68072°E) is indicated with a letter X and the outlet is indicated with a letter Y (13.40050°N; 39.68125°E).

Figure 3. Sampling site (indicated with red arrow) and sampling of the modern sample (M), just upstream of a newly built check dam in the May Tsimble channel.

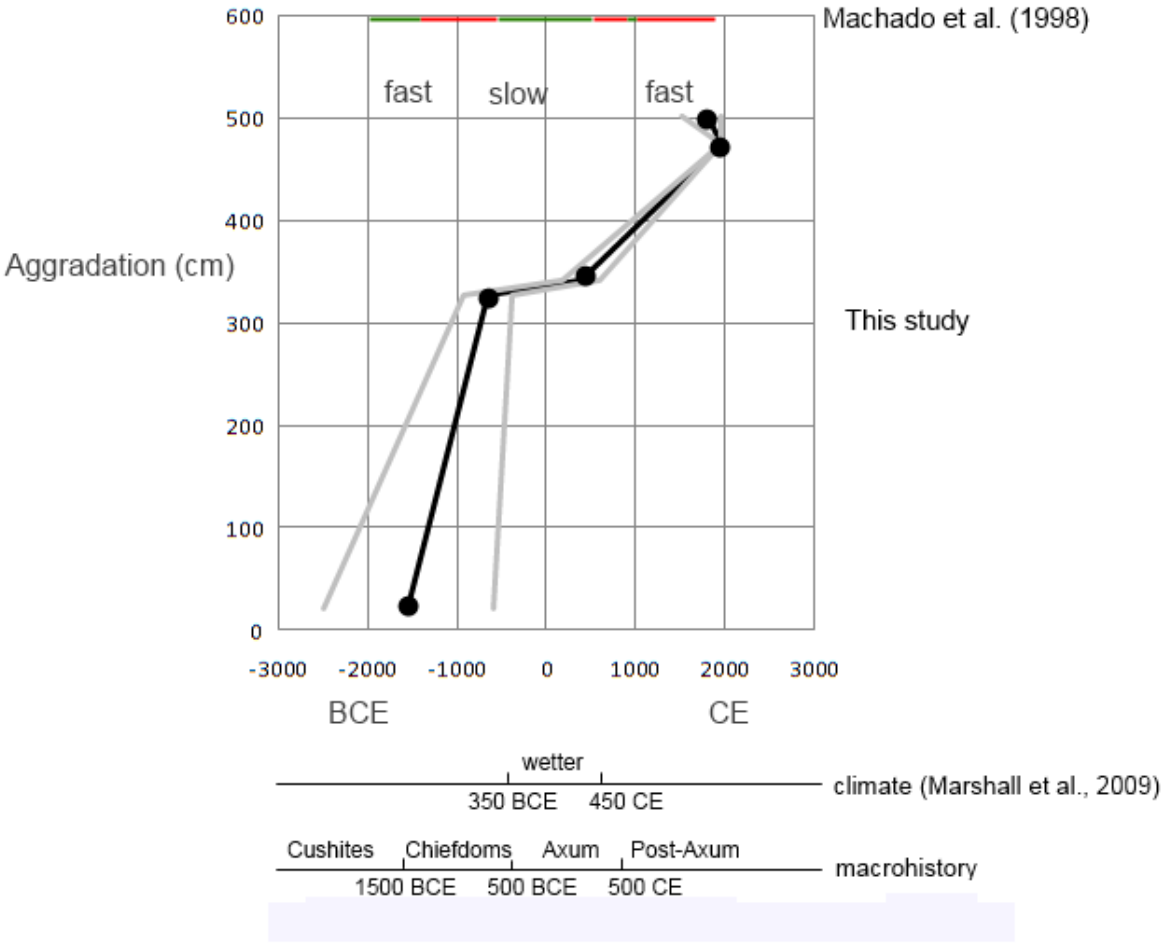

761 Figure 4. Measured deposition ages (black dots) of sediment (BCE and CE) with errors (grey
762 lines) as corrected for the residual age, and floodplain aggradation above the Antalo limestone
763 base (cm) with indication of fast and slow aggradation rates. The degradation periods
764 identified by Machado et al. (1998) are indicated with red bars, the vertisol stabilization
765 periods are indicated with green bars. Important climatic and historical changes are also
766 indicated.

767

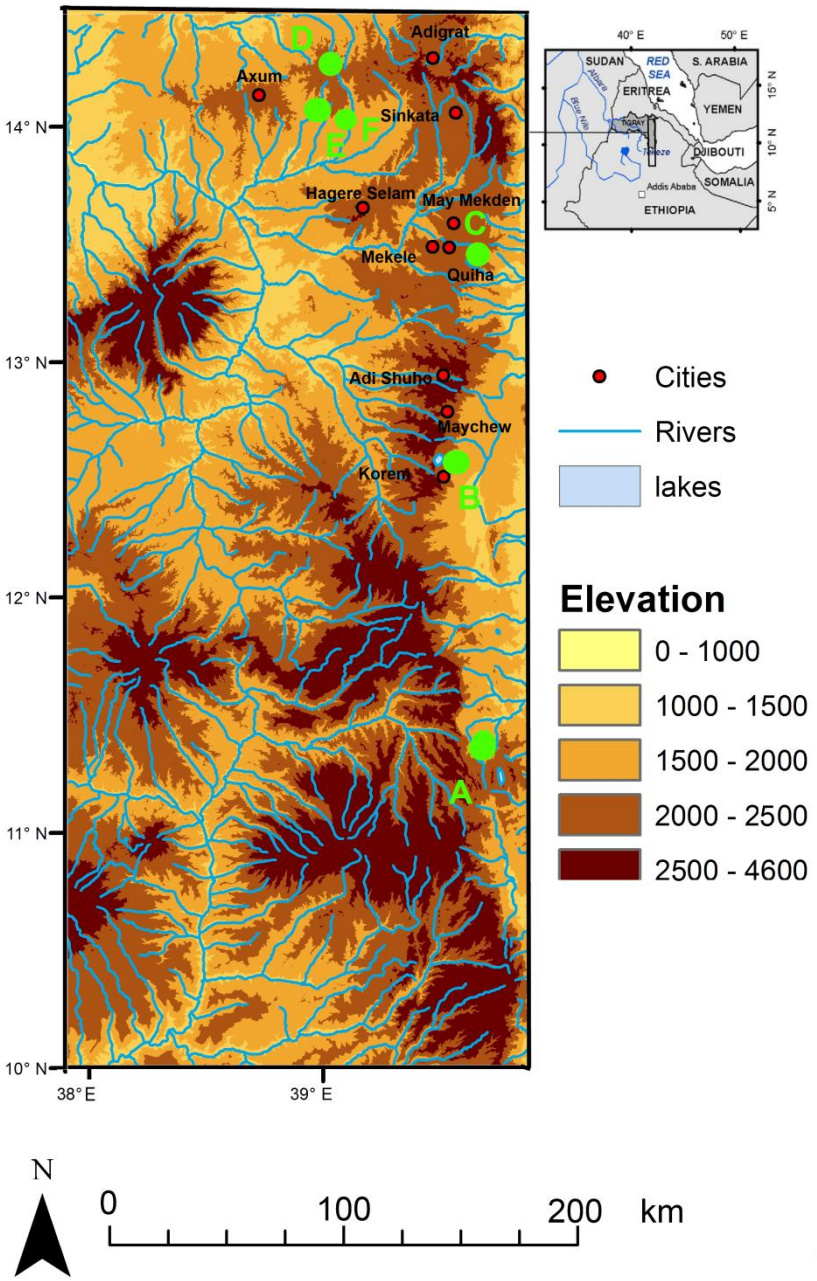

768

769 Figure 5. Map of all mentioned paleo environmental records in the Northern Highlands, with
770 A = Lake Hayk (Darbyshire et al., 2003; Lamb et al., 2007), B = Lake Ashenge (Marshall et
771 al., 2009), C = May Tsimble (this study), D = Yeha (Pietsch & Machado, 2012), E = Adwa
772 (Machado et al., 1998), F = Wechi and May Kinetal (Machado et al., 1998).

773

774

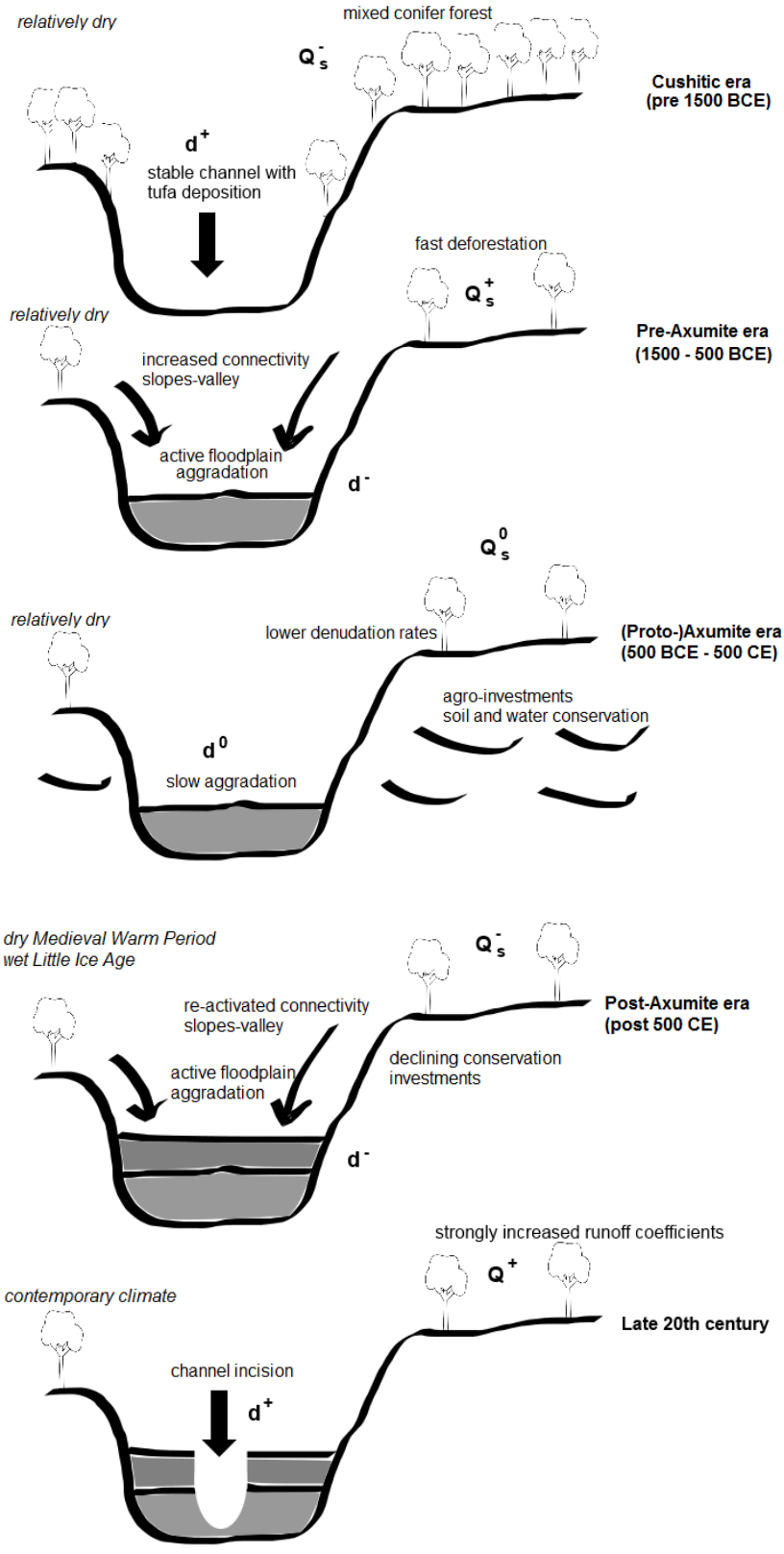

Figure 6. Conceptual geomorphic model of stream and landscape evolution. The figure indicates channel aggradation (d^-), increase in sediment supply (Q_s^+), channel incision (d^+), increase in water runoff (Q^+) and a decrease in sediment load (Q_s^-). Indication of 0 stands for a stable situation.

781

782

783 Figure 7. (a) Base of the sequence (indicated by stick) (left); and (b) small waterfall parallel to
784 our study site, with travertine identified (indicated by red arrow) (right).

785

786

787 Table 3. OSL data for single samples and aggradation depths (above the Antalo limestone
788 base).

Description	Lab Code and Field Code	Burial Depth (cm)	Water Content (%)	Paleodose (Gy)	±	Dose Rate (Gy/ka)	±	OSL age (years before 2014)	Age after correction	±	Aggradation depth (above Antalo limestone base) (cm)
Residual age	X6431 (M)	34	13.3	0.48	0.2	1.22	0.07	<400	2010 CE		
Right upper terrace	X6432 (β)	150	13.6	0.27	0.24	1.45	0.07	<200	~ 1960 CE		474
Left upper terrace	X6433 (δ)	99	15.4	0.62	0.35	1.22	0.06	510	1804 CE	290	502
Top of the profile pit	X6435 (ε)	28	17.8	2.34	0.2	1.22	0.07	1920	394 CE	210	342
Left lower subterrace pit	X6434 (γ)	132	11.0	3.63	0.26	1.22	0.06	2970	656 BCE	270	326
Bottom of the aggradation	X6437 (α)	370	19.4	3.21	0.78	0.83	0.04	3860	1546 BCE	950	21
Bottom of the profile pit	X6436 (ζ)	120	14.5	27.27	4.98	1.09	0.05	24990	22676 BCE	4760	250

789
790
791
792
793

794 Table 4. Regional rainfall regime changes and land cover changes in the North Ethiopian
795 Highlands derived from Lake Hayk and Lake Ashenge; degradation derived from Wechi,
796 Adwa, May Kinetal and May Tsimble; and macrohistory.

797 *See separate document*

798

799

APPENDIX

K, Th and U concentrations, as determined by Induced Coupled Plasma Mass Spectroscopy / Atomic Emission Spectroscopy using a fusion sample preparation technique.

	Unit	X6431	X6432	X6433	X6434	X6435	X6436	X6437
Grain sizes								
Min. grain size	(mm)	180	180	180	180	180	180	180
Max . grain size	(mm)	255	255	255	255	255	255	255
Measured concentrations								
Standard fractional error	(%)	5	5	5	5	5	5	5
% K	(%)	0.697	0.905	0.672	0.706	0.755	0.64	0.43
Error (% K)	(%)	0.035	0.045	0.034	0.035	0.038	0.032	0.022
Th	(ppm)	3	4.3	3.5	3.1	3.4	2.9	2.3
Error (Th)	(ppm)	0.15	0.215	0.175	0.155	0.17	0.145	0.115
U	(ppm)	1.1	1.3	1.3	1.1	1.1	1	1.2
Error (U)	(ppm)	0.055	0.065	0.065	0.055	0.055	0.05	0.06

Equivalent doses, cosmic doses, moisture content, total dose rate and age estimates.

	Unit	X6431	X6432	X6433	X6434	X6435	X6436	X6437
De	(Gy)	(0.48)	(0.27)	0.62	3.63	2.34	27.27	3.21
uncertainty		0.19	0.24	0.35	0.27	0.21	5.01	0.77
Cosmic dose calculations								
Depth	(m)	0.34	1.5	0.99	1.32	0.28	1.2	3.7
error	(m)	0.05	0.05	0.05	0.05	0.05	0.05	0.05
Average overburden density	($g.cm^3$)	1.9	1.9	1.9	1.9	1.9	1.9	1.9
error	($g.cm^3$)	0.1	0.1	0.1	0.1	0.1	0.1	0.1
Latitude		13	13	13	13	13	13	13
Longditude		40	40	40	40	40	40	40
Altitude	(m a.s.l.)	2052	2023	2023	2020	2020	2019	2019
Geomagnetic	latitude	9	9	9	9	9	9	9
Dc	(Gy/ka), 55N G.lat, 0 km Alt.	0.201	0.172	0.184	0.176	0.202	0.179	0.131
error		0.033	0.014	0.016	0.014	0.039	0.015	0.01
Cosmic dose rate	(Gy/ka)	0.249	0.213	0.228	0.218	0.25	0.222	0.162
error	0.041	0.017	0.02	0.018		0.048	0.019	0.012
Moisture content								
Measured water	(% of wet sediment)	13.27	13.64	15.38	11	17.78	14.54	19.36
Moisture	(water/wet sediment)	0.13	0.14	0.15	0.11	0.18	0.15	0.19
error	0.03	0.03	0.03	0.03		0.03	0.03	0.03
Total dose rate	(Gy/ka)	1.216	1.449	1.216	1.224	1.218	1.091	0.831
error		0.07	0.075	0.06	0.062	0.075	0.054	0.039
OSL age estimate	(yr before 2014)	(<400)	(<200)	510	2970	1920	24990	3860
error				290	270	210	4760	950

805

806